AIP | Applied Physics Letters

The role of structural properties on deep defect states in Cu2ZnSnS4 studied by photoluminescence spectroscopy

M. Grossberg, J. Krustok, J. Raudoja, and T. Raadik

Citation: Appl. Phys. Lett. **101**, 102102 (2012); doi: 10.1063/1.4750249
View online: http://dx.doi.org/10.1063/1.4750249
View Table of Contents: http://apl.aip.org/resource/1/APPLAB/v101/i10
Published by the American Institute of Physics.

The role of structural properties on deep defect states in Cu_2ZnSnS_4 studied by photoluminescence spectroscopy

M. Grossberg,[a] J. Krustok, J. Raudoja, and T. Raadik
Tallinn University of Technology, Ehitajate Tee 5, 19086 Tallinn, Estonia

(Received 19 June 2012; accepted 21 August 2012; published online 4 September 2012)

In this study, we investigated the photoluminescence (PL) properties of Cu_2ZnSnS_4 polycrystals. Two PL bands at 1.27 eV and 1.35 eV at T = 10 K were detected. Similar behaviour with temperature and excitation power was found for both PL bands and attributed to the band-to-impurity recombination. Interestingly, the thermal activation energies determined from the temperature dependence of the PL bands coincide. With the support of the Raman results, we propose that the observed PL bands arise from the band-to-impurity-recombination process involving the same deep acceptor defect with ionization energy of around 280 meV but different Cu_2ZnSnS_4 phase with different bandgap energy. © *2012 American Institute of Physics*.
[http://dx.doi.org/10.1063/1.4750249]

Cu_2ZnSnS_4 (CZTS) is considered as non-toxic and low-cost absorber material for solar cells, which has optimal direct bandgap energy for solar energy absorption and high absorption coefficient. Current record of the solar energy conversion efficiency of CZTS based solar cells is 8.4%.[1] Besides lot of effort that has been put into developing devices based on CZTS absorbers, there is still far too little information about the fundamental physical properties of this compound that is clearly also limiting the improvement of device properties.

In low-temperature photoluminescence (PL) studies, a broad and asymmetric photoluminescence band at around 1.3 eV has been detected in many papers;[2–7] however, the origin of this PL band is still not clear. Tanaka *et al.*[3] have attributed it to donor-acceptor pair (DAP) recombination with a thermal activation energy of $E_T = 48$ meV in S-poor CZTS single crystals. From the same group, the origin of the 1.3 eV PL for the stoichiometric thin films was attributed to DAP recombination with $E_T = 39$ meV, and for Cu-poor and Zn-rich thin films to DAP recombination with $E_T = 59$ meV.[4] Leitao *et al.*[5] observed PL band at 1.24 eV in Cu-poor and Zn-rich thin films and attributed it to tail states created by potential fluctuations. In the other papers,[2,6,7] detailed analysis of this PL band is not presented. In summary, there is no clear model related to this PL band at 1.3 eV in CZTS.

Hönes *et al.*[2] have also observed the edge emission in CZTS and proposed a defect related recombination model for CZTS involving shallow defect levels—two shallow acceptor states at 10 ± 5 meV and 30 ± 5 meV, and a donor state at 5 ± 3 meV. Shallow defects with an ionization energies of $E_T = 69 \pm 4$ meV, 27 ± 3 meV, and 7 ± 2 meV have also been found in PL studies of $Cu_2ZnSnSe_4$ (CZTSe).[8,9]

The defect formation energies of CZTS calculated by using first-principles calculations were published by Chen *et al.*[10] They found that the p-type conductivity of CZTS is mainly determined by a Cu_{Zn} acceptor defect with $E_A = 0.12$ eV that was also found experimentally by admittance spectroscopy in monograin layer solar cells based on CZTS.[11] However, no other deep defects have been detected so far in CZTS.

There has also been discussion about the crystal structure of CZTS, whether it is a kesterite or stannite. These two crystallographic forms are very close with the only difference in the distribution of the cations in the tetrahedral sites. The general consensus is that the kesterite structure is the ground-state structure, but according to the calculations made by Chen and co-workers[10] the energy difference between kesterite and stannite is only about 3 meV per atom,[12] indicating that the disorder in the cation sublattice may occur under standard growth conditions. The disorder is predicted to affect the bandgap of the material and Chen *et al.*[12] have determined the bandgap energy difference of 0.12 eV for the kesterite and stannite phases in CZTS, the latter being smaller. Neutron diffraction measurements by Schorr *et al.*[13,14] also showed that a partially disordered kesterite structure can exist, in which the atoms in the Cu/Zn (001) layer are disordered, while atoms in the Cu/Sn (001) layer reside in their original positions. If the displacement occurs randomly in the Cu + Zn layers, the disordered kesterite phase results in an effective symmetry equivalent to the stannite structure. It is difficult to assign the crystal structure based on x-ray diffraction techniques because the difference in the scattering cross-sections between Cu and Zn is small and hence similar diffraction patterns are produced for kesterite, stannite, and all related partially disordered phases.[15] Though the vibrational spectra of these phases are also similar, according to calculations by Gürel *et al.*[16] and Khare *et al.*[17] there is a difference at least in A_1 phonon modes of kesterite and stannite CZTS. This difference in peak positions or their coexistence can be detected in the case of very narrow Raman peaks. Khare *et al.*[17] have detected experimentally the A_1 phonon modes of kesterite and stannite CZTS and determined a difference of 3 cm^{-1} in their peak positions. In the present Raman and PL study of polycrystalline CZTS, we show a coexistence of kesterite and disordered kesterite phases in CZTS and report a role of these phases on deep PL bands.

[a]Author to whom correspondence should be addressed. Electronic mail: Maarja.Grossberg@ttu.ee.

Cu_2ZnSnS_4 polycrystalline powder was synthesized from the metallic precursor powders with the purity of 99.9%. The metal powders and sulphur were mixed properly in mortir. Then, the powder was inserted into quartz ampoule that was degassed and sealed. The ampoule with the material was kept at 1000 °C for 50 h and then quenched into water. To obtain Cu-rich CZTS powder, Cu_2S and S were added to the initial CZTS powder. The powder was again mixed properly in mortir, inserted into quartz ampoule that was degassed and sealed. The ampoule with the material was kept at 550 °C for 170 h to obtain equilibria of CZTS and then cooled with the furnace slowly during 40 h to 100 °C. The composition of the CZTS polycrystals was analysed by using energy dispersive spectroscopy (EDS) and was found to be slightly Cu-rich.

The room temperature Raman spectra were recorded by using a Horiba's LabRam HR spectrometer equipped with a multichannel CCD detection system in the backscattering configuration. In micro-Raman measurements, the incident laser light with the wavelength of 532 nm was used. For PL measurements, the samples were mounted in the closed-cycle He cryostat and cooled down to 10 K. The 405 nm laser line was used for PL excitation.

Fig. 1 presents room-temperature Raman spectrum of CZTS polycrystals. Raman peaks were determined by fitting the spectrum with Lorentzian curves and were detected at 98, 142, 168, 252, 263, 288, 334.3, 338.6, 347, 355, and 365 cm^{-1}. The origin of these Raman peaks except for the 334.3 cm^{-1} has been studied before[17,18] and is not overwritten here. The full width at half maximum of the A_1 peak is only $W = 2.6\,cm^{-1}$. The presence of an additional Raman peak at 334.3 cm^{-1} giving a shoulder to the CZTS A_1 peak at 338.6 cm^{-1} is observed. This shoulder peak was also detected by Khare *et al.*[17] For the shoulder peak in current study, $W = 9.9\,cm^{-1}$ and its intensity relative to the A_1 peak intensity varies from point to point on the sample. It has to be mentioned that this peak at 334.3 cm^{-1} cannot be attributed to some of the known binaries and ternaries that can be possibly formed during the growth of CZTS. According to the calculations by Gürel *et al.*,[16] the A_1 mode frequencies of kesterite and stannite CZTS are 335.2 cm^{-1} and 332.7 cm^{-1}, respectively. According to the calculations by Khare *et al.*,[17] the A_1 mode frequencies of kesterite and stannite CZTS are 340.04 cm^{-1} and 334.08 cm^{-1}, respectively. The difference in the A_1 Raman modes in the present study is 4.3 cm^{-1} that is quite close to the calculated differences of 2.5 cm^{-1} (Ref. 16) and 6 cm^{-1} (Ref. 17). However, the width of the 334.3 cm^{-1} peak is quite large ($W = 9.9\,cm^{-1}$), indicating a disorder in the phase related to this peak. It should be mentioned that the calculations in Refs. 16 and 17 were made for pure kesterite and stannite phases. Therefore, we propose that the shoulder peak at 334.3 cm^{-1} can be attributed to the disordered kesterite which can also be close to the stannite phase. However, we do not know the exact atomic displacements and cannot say which kind of ordering is present in the studied CZTS polycrystals.

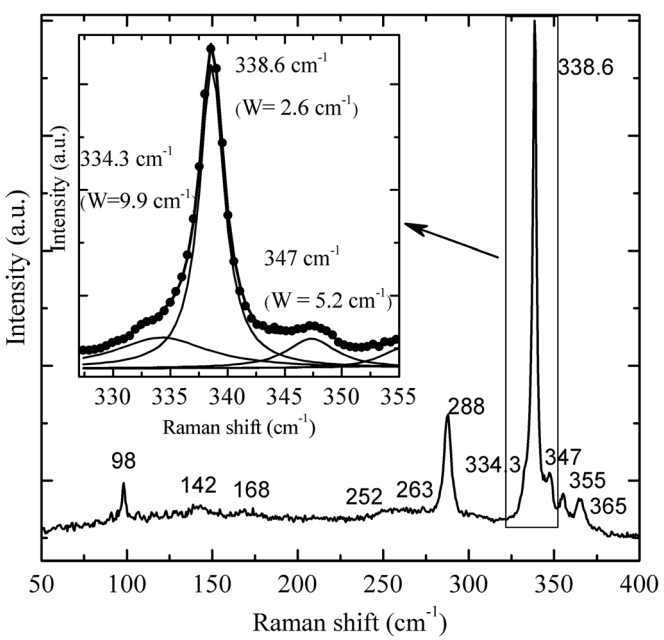

FIG. 1. Raman spectrum of CZTS polycrystals. The fitting result for the A_1 peak is shown on the inset graph, where the original spectrum is presented with symbols. A shoulder peak at 334.3 cm^{-1} is observed.

The low-temperature PL spectrum of CZTS polycrystals is presented in Fig. 2. The PL spectrum consists of two bands at 1.27 eV and 1.35 eV. The fittings of these bands showed that they are slightly asymmetrical and have an exponential slope on the low-energy side. For the fitting, empirical asymmetric double sigmoidal function was used (see details in Ref. 19). The full width at the half maximum of these PL bands is only 100 meV being the narrowest presented for the PL band at 1.3 eV so far. In order to determine the recombination processes, the laser power and temperature dependencies of the PL spectrum were measured.

The laser power dependence of the low-temperature PL spectrum revealed a strong blue shift of 15 meV per decade with increasing excitation power of both bands. This behaviour is typical for recombination in heavily doped semiconductors where potential fluctuations are present.[8,19–21]

The temperature dependence of the PL spectrum was measured in the temperature range of 10–280 K. The thermal activation energies were determined from the Arrhenius plot (Fig. 3). The linear dependence of $\ln I(T)$ versus 1000/T at high temperatures was fitted by using theoretical expression

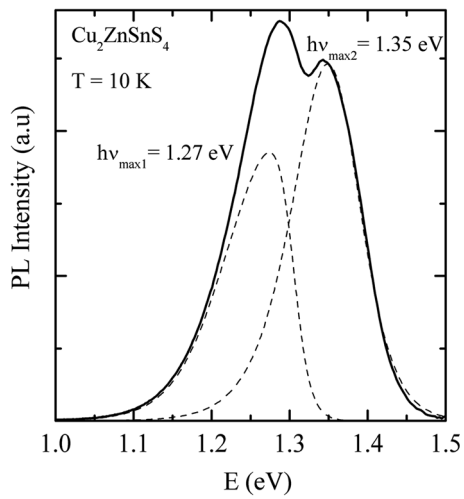

FIG. 2. Low-temperature PL spectrum of CZTS polycrystals together with the fitting result.

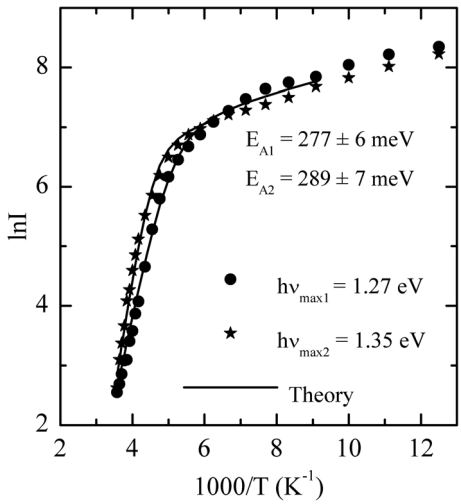

FIG. 3. Arrhenius plot derived from the temperature dependencies of the PL spectra of CZTS polycrystals. Thermal activation energies 289 ± 7 meV and 277 ± 6 meV were obtained for the PL bands at 1.35 eV and 1.27 eV, respectively. Solid lines present the fitting of the high temperature experimental data with the theoretical expression.[22]

for discrete energy levels proposed in Ref. 22. Interestingly, both PL bands showed similar behaviour with temperature and even similar thermal activation energies 289 ± 7 meV and 277 ± 6 meV were obtained. The temperature dependence of the peak positions of the PL bands (see Fig. 4.) more or less follows the temperature dependence of the bandgap energy as presented in Ref. 23.

The asymmetric shape of the PL bands and the large blue shift with laser power are common to compensated heavily doped semiconductors, where spatial potential fluctuations are present.[8,19–21] The conditions of heavy doping in present case originate from the high concentration of native defects that is often observed in multinary compounds.[8,19,21] The potential fluctuations will lead to a local perturbation of the band structure, thus broadening the defect level distribution and forming band tails. The average depth of the potential fluctuations γ was determined from the exponential slope of the low-energy side $I(E) \sim \exp(-E/\gamma)$ (see details in Ref.

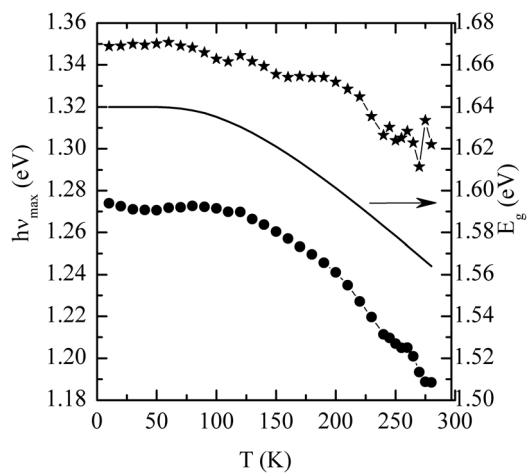

FIG. 4. Temperature dependence of the peak positions of the PL bands presented together with the temperature dependence of the bandgap energy (solid line) of CZTS as found by Sarswat and Free[23] by using the Bose-Einstein model.

20) of the PL bands and was found to be around 11 meV that is much smaller than presented in the study by Leitao *et al.*[5] where the depth of the fluctuations was found to be 172 ± 2 meV. It is also smaller than we found in CZTS monograins (47 meV) where the flux material (potassium iodide) leaves some residues in the material.[6] Keeping in mind that CZTS is a p-type material, the behaviour of the PL bands with temperature and laser power indicates that the emission arises from the band-to-impurity (BI) recombination that involves an acceptor state that is deep enough not to overlap with the valence band tail[8,20] that does not extend deep into the band gap due to small depth of the fluctuations (11 meV). The ionization energies of the acceptor defects involved in the recombination are 289 ± 7 meV and 277 ± 6 meV for the PL bands at 1.35 eV and 1.27 eV, respectively.

With the support of the Raman results, we propose that the observed PL bands arise from the BI-recombination process involving the same acceptor defect with ionization energy of around 280 meV but different CZTS phase. Since according to Chen *et al.*,[12] the bandgap energy difference of the kesterite and stannite phases in CZTS is 0.12 eV, the latter being smaller, we propose that the PL band at 1.27 eV originates from the disordered kesterite and the PL band at 1.35 eV from the pure kesterite CZTS. Since the energy differenece of the PL bands (0.08 eV) is smaller than the calculated bandgap energy difference for kesterite and stannite phases, the PL band at 1.27 eV should be attributed to the disordered kesterite phase.

According to the theory of heavily doped semiconductors,[20] at low temperatures the BI-band is located at $h\nu_{max} = E_g - I_a$, where E_g is the bandgap energy and I_a is the ionization energy of an acceptor defect. As a result, for the kesterite CZTS we obtain bandgap energy of $1.35 + 0.289 = 1.639$ eV that is in accordance with the results obtained in Ref. 23 for T = 0 K, see Fig. 4.

According to the calculations by Chen *et al.*,[10] the observed acceptor defect with the ionization energy around 280 meV could be Cu_{Sn}, Zn_{Sn}, V_{Zn}, or V_{Sn}. The lowest formation energies were found for Cu_{Sn} and Zn_{Sn} that should therefore be taken as the most probable candidates. Since we have slightly Cu-rich material, we propose Cu_{Sn} could be the observed deep acceptor defect.

In conclusion, two PL bands at 1.27 eV and 1.35 eV at T = 10 K were detected in the PL spectrum of CZTS polycrystals. Similar behaviour with temperature and excitation power was found for both PL bands and attributed to the BI-recombination. Thermal activation energies of 289 ± 7 meV and 277 ± 6 meV were obtained for the PL bands at 1.35 eV and 1.27 eV, respectively. With the support of the Raman results, we propose that the observed PL bands arise from the BI-recombination process involving the same deep acceptor defect with ionization energy of around 280 meV but different CZTS phase. The PL band at 1.35 eV arises from the kesterite CZTS and the PL band at 1.27 eV from disordered kesterite phase. We propose that the observed deep acceptor defect could be Cu_{Sn}.

This work was supported by the Estonian Science Foundation Grants G-8282 and ETF 9369, by the target financing

by HTM (Estonia) No. SF0140099s08, and Estonian Centre of Excellence in Research, Project TK117.

[1]B. Shin, O. Gunawan, Y. Zhu, N. A. Bojarczuk, S. J. Chey, and S. Guha, "Thin film solar cell with 8.4% power conversion efficiency using an earth-abundant Cu_2ZnSnS_4 absorber," Prog. Photovoltaics (2011).
[2]K. Hönes, E. Zscherpel, J. Scragg, and S. Siebentritt, Physica B **404**, 4949 (2009).
[3]K. Tanaka, Y. Miyamoto, H. Uchiki, K. Nakazawa, and H. Araki, Phys. Status Solidi A **203**, 2891 (2006).
[4]Y. Miyamoto, K. Tanaka, M. Oonuki, N. Moritake, and H. Uchiki, Jpn. J. Appl. Phys., Part 1 **47**, 596 (2008).
[5]J. P. Leitao, N. M. Santos, P. A. Fernandes, P. M. P. Salome, A. F. da Cunha, J. C. Gonzalez, G. M. Ribeiro, and F. M. Matinaga, Phys. Rev. B **84**, 024120 (2011).
[6]M. Grossberg, J. Krustok, J. Raudoja, K. Timmo, M. Altosaar, and T. Raadik, Thin Solid Films **519**, 7403 (2011).
[7]H. Yoo, J. H. Kim, and L. Zhang, Curr. Appl. Phys. **12**, 1052 (2012).
[8]M. Grossberg, J. Krustok, K. Timmo, and M. Altosaar, Thin Solid Films **517**, 2489 (2009).
[9]F. Luckert, D. I. Hamilton, M. V. Yakushev, N. S. Beattie, G. Zoppi, M. Moynihan, I. Forbes, A. V. Karotki, A. V. Mudryi, M. Grossberg, J. Krustok, and R. W. Martin, Appl. Phys. Lett. **99**, 062104 (2011).
[10]S. Chen, J.-H. Yang, X. G. Gong, A. Walsh, and S.-H. Wei, Phys. Rev. B **81**, 245204 (2010).
[11]E. Kask, T. Raadik, M. Grossberg, R. Josepson, and J. Krustok, Energy Procedia **10**, 261 (2011).
[12]S. Chen, X. G. Gong, A. Walsh, and S. H. Wei, Appl. Phys. Lett. **94**, 041903 (2009).
[13]S. Schorr, H.-J. Hoebler, and M. Tovar, Eur. J. Mineral. **19**, 65 (2007).
[14]S. Schorr, Sol. Energy Mater. Sol. Cells **95**, 1482 (2011).
[15]S. Chen, A. Walsh, Y. Luo, J. H. Yang, X. Gong, and S. H. Wei, Phys. Rev. B **82**, 195203 (2010).
[16]T. Gürel, C. Sevik, and T. Cagin, Phys. Rev. B **84**, 205201 (2011).
[17]A. Khare, B. Himmetoglu, M. Johnson, D. J. Norris, M. Cococcioni, and E. S. Aydil, J. Appl. Phys. **111**, 083707 (2012).
[18]P. A. Fernandes, P. M. P. Salome, and A. F. da Cunha, J. Alloys Compd. **509**, 7600 (2011).
[19]J. Krustok, H. Collan, M. Yakushev, and K. Hjelt, Phys. Scr. **T79**, 179 (1999).
[20]A. P. Levanyuk and V. V. Osipov, Sov. Phys. Usp. **24**, 187 (1981).
[21]A. Jagomägi, J. Krustok, J. Raudoja, M. Grossberg, M. Danilson, and M. Yakushev, Physica B **337**, 369 (2003).
[22]J. Krustok, H. Collan, and K. Hjelt, J. Appl. Phys. **81**, 1442 (1997).
[23]P. K. Sarswat and M. L. Free, Physica B **407**, 108 (2012).